Asian Journal of Chemistry; Vol. 27, No. 5 (2015), 1589-1592

ASIAN JOURNAL OF CHEMISTRY

http://dx.doi.org/10.14233/ajchem.2015.17382

Molecular Mechanism of MDM2 with Novel Small Inhibitor Recognition Explored by Molecular Dynamics Simulation and Free Energy Analysis

HUI LI[1,*], SHI-KUI HU[1,2], XU WEN[1,2], XI-HAI LIANG[1,2] and HONG ZENG[1,2]

[1]School of Life Science, Liaoning University, Shenyang 110036, Liaoning Province 110036, P.R. China
[2]School of Life Science and Bio-Pharmaceutics, Shenyang Pharmaceutical University, Shenyang 110016, Liaoning Province 110016, P.R. China

*Corresponding author: E-mail: zhiyao77@126.com

Received: 13 February 2014; *Accepted*: 6 May 2014; *Published online*: 20 February 2015; AJC-16849

P53 is a powerful anti-tumoral molecule which is frequently inactivated by its major negative regulator, MDM2. Inhibition of p52-MDM2 interaction is increasingly gaining interest in cancer therapy and drug design. Molecular docking coupled with molecular dynamics and molecular mechanics generalized. Born surface area (MM-GBSA) method was performed to investigate the binding mechanisms of compound 9c to MDM2. These results show that the van der Waals energy is the largest component of the binding free energy for the MDM2-9c complex, which is consistent with the experimental results. In addition, analysis of individual reside contribution and protein-ligand binding mode show that there are more space and opportunity for derivatization at the C-2 and C-3 position, respectively. It is expected the results obtained from this study will be valuable for future rational design of novel and potent MDM2 inhibitors targeting the p53-MDM2 interaction.

Keywords: MEM2, Molecular simulation, Molecular dynamics, p53.

INTRODUCTION

The p53 protein as a tumor suppressor plays an important role in cellular mechanisms in cell arrest, apoptosis, DNA repair and senescence. Once active under cellular stress in the form of DNA damage, onceogenic activation, or hypoxia, p53 can accumulate in the nucleus and exert supper antitumor effort through two distinct and parallel pathways[1-3]. Indeed, about 50 % of all human cancers harbor mutations or deletions in p53 gene[4-7]. However, in some the remaining of human malignancies, the functions of wide-type p53 are regulated by an over expression or an amplification of human murine double minute-2 gene product (MDM2, or HDM2 for the human congener)[8-11].

MDM2 is an important negative regulator of the activity and stability of p53, which directly forms a protein-protein interaction with p53, thus blocking p53 transcriptional activity[12-15]. The major domain of MDM2 consist of several conserved domains including an N-terminal domain that binds the α-helix from the N-terminal transactivation domain of p53, an acidic domain capable of interacting with p300 and the tumor suppressor p14/ARF and a RING figure domain that harbors the E3 ligase activity responsible for p53 ubiquitination[16]. Therefore, reactivation of p53 pathway holds great promise for cancer therapy by inhibiting the MMD2-p53 interaction[17,18].

Recent studies have shown that restoring endogenous p53 activity can halt the growth of cancerous tumors in animals. Many researchers thus pay attention to the investigation of the MDM2-p53 interaction and the design of their interaction inhibitors[19-24]. In recent decades, the structural basis for the interaction of p53 with the N-terminal domains of MDM2 is well understood and several different small molecules which inhibit p53-MDM2 interactions have been designed[25-32]. However, a limited number of compounds can efficiently inhibit the p53-MDM2 interaction, among which potent inhibitors reported first were Nutlin-3a, MI-219 and AM-8553[33-36]. In order to provide valuable information about the structure-affinity relationship of the binding complex and design potent inhibitors, it is necessary to understanding the binding mechanisms of non-peptide inhibitors to MDM2 at the atomic level. Recently, a few computational studies have been performed to investigate the p53-MDM2 system[35-40]. In this work, we selected a non-peptide inhibitor **9c** having a dihydroimidazothiazole scaffold to investigate the interaction mechanisms of the compound **9c** with MDM2 with IC50 values of 0.26 um[41]. Fig. 1 depicted the structures of the compound **9c** and points out the parts imitating the three residues of p53: Phe19, Trp23 and Leu26, inserting into a hydrophobic groove in MDM2.

Binding free energy calculations and analysis have been proven to serve as a powerful and valuable tool for under

standing the binding mechanisms of ligands to proteins[42-44]. Furthermore, MM-GBSA method has been used successfully in explaining protein-protein and protein-ligand interaction[45-53]. In this study, we propose an integrated computational protocol combing molecular docking, molecular dynamics and free energy calculations to gain insights into the binding mode. In addition, we also expect the knowledge gained from this study can be used in identification and structure based design of the potent inhibitors inhibiting the interaction of p53 to MDM2.

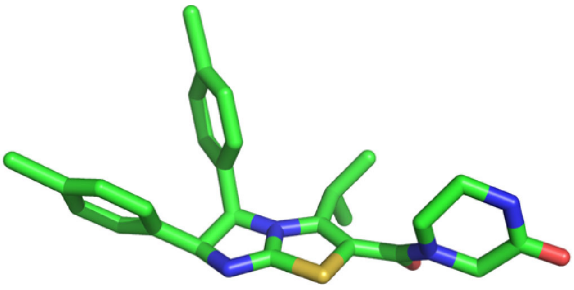

Fig. 1. Structure of the inhibitor dihydroimidazothiazoles (**9c**)

EXPERIMENTAL

As shown in Fig. 1, the structure of the compound **9c** was constructed using the pymol sofware[54]. The crystal structure of MDM2 was extracted from the Protein Data Bank (PDB ID: 4ERE)

Molecular docking: The AutoDock 4.2[55] was used to perform docking calculations. The compunds **9c** was docked to the entire surface of the MDM2. Flexible torsions in the ligands were assigned with the biopolymer module and all dihedral angles were allowed to rotate freely. The graphical front-end, AutoDockTools, was used to add polar hydrogens and partial charges for protein using the Kollman United Atom charges. Atomic solvation parameters and fragmental volumes for the proteins were assigned using the add-sol utility in the program package. The docking procedure was applied to the whole protein target with a grid spacing of 0.375 Å. Affinity grid fields were generated using the auxiliary program AutoGrid. The Lamarckian genetic algorithm (LGA) was used to find the appropriate binding positions, orientations and conformations of the ligands. Default parameters were used, except for the number of generations which was set at 100. The resulting data were taken from docking experiments in which the lowest total docking energy was obtained.

Molecular dynamics simulation: All simulations were performed by using the sander module of the Amber12 software[56]. The leap module in Amber12 package was used to add all missing amino acid residues and hydrogen atoms. All of the crystal water molecules were maintained in the starting model. The ff99SB and general amber force field (GAFF)[57] were used for the proteins and the inhibitors, respectively. The systems were subsequent solvated in a rectangular box of TIP3P explicit water model with a minimum 12 Å distance between any protein atoms and the box boundaries. To neutralize the modes, an appropriate number of chloride counter ions were added.

Prior to molecular dynamics simulation, a series of minimizations were performed. All the water molecules were first minimized while restraining the protein-atomic positions with a harmonic potential. The systems were energy minimized without restraints for another 2000 steps using a combination of the steepest descent and conjugated gradient methods. After the systems were gradually heated from 10 to 300 K over 100 ps using the NVT ensemble, a 1 ns simulation at 1 atm and 300 k with NPT ensemble was carried out to equilibrate the systems. For production runs, molecular dynamics simulations were performed in the NPT ensemble for 50 ns.

For all simulations, all bonds involving hydrogen atoms were constrained using the SHAKE algorithm[58]. A time step of 2 fs and a non-bond interaction cut-off radius of 10 Å were used. The particle-mesh Ewald (PME) was employed to calculate the long-range electrostatic interactions[59,60]. During the sampling process, a snapshot of the system was saved every 5 ps for further analysis.

MM-GBSA calculation: In this work, a total number of 200 snapshots were taken from the last 2 ns molecular dynamics simulations to analyze binding free energy using MM-GBSA method and nmod module in Amber12 software.

RESULTS AND DISCUSSION

Molecular docking analysis: The compound **9c** was docked onto the active sites of MDM2 to locate the potential binding modes. According to most favorable binding free energy and the cluster conformation analysis, the predicted docked complex is selected and subsequently subjected to perform molecular dynamics simulations with Amber99 force field.

The crystal structures of MDM2 bound to various peptide and small-molecule ligands have been solved, demonstrating the key shape-filling and hydrophobic interactions and revealing the primary interactions involve three hydrophobic residues (Trp23, Leu26, Phe19). Many series of compounds developed as potent MDM2-p53 inhibitors, such as Nutlin-3, MI-219 and AM-8553, are designed to mimic the side chain of the Trp23, Leu26 and Phe19 residues in p53 and have shown *in vivo* antitumor activity. Therefore, the compound **9c** illustrated with an estimated docking configuration was posed by superposition to the co-crystal structure of MDM2 (PDB ID: 1RV1) in order to reveal whether the compound **9c** can mimic the spatial orientation of the side chains of the triad residues in p53 peptide. As shown in Fig. 2, two chlorophenyl groups and the *iso*-propyl group of compound **9c** can mimic the side chain of Trp23, Leu26 and Phe19, respectively.

Molecular dynamics simulations: To understand the dynamic stability of the complex system, the root mean square deviation (RMSD) values of the heavy atoms compared with the starting coordinates were calculated and plotted in Fig. 3. As seen from Fig. 3, the trajectory of the complex maintains quite stable up to about 5 ns and then it remains stable throughout the following 15 ns of the simulation. This result indicates that the molecular dynamics simulation trajectories are reliable for the post analyses. The average structure of the system from the last 2 ns of simulation was calculated and shown in Fig. 4. We observe that the two chlorophenyl groups sit deeply in the Leu26 and Trp23 subpocket, respectively. In addition, the Phe19 subpocket is partially occupied by the 6-membrered rings and the *iso*-propyl group. Miyazaki *et al.*[41] suggested there seems to be more space and opportunity for derivatization

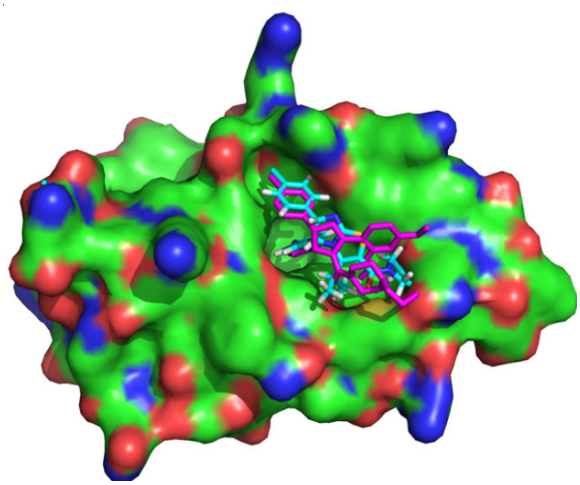

Fig. 2. Predicted binding model of compound **9c** in blue superposed on the crystal structure (PDB code: 1RV1) by docking calculation

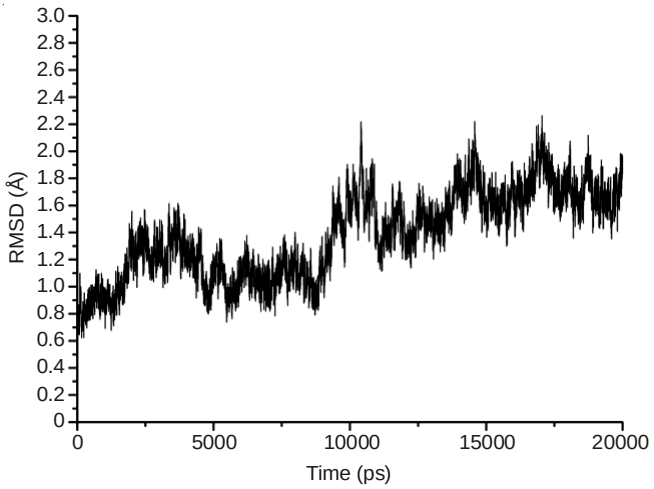

Fig. 3. Root mean squre derivations (RMSD) of Cα atoms relative to their initial minimized complex structures as function of time

at the C-2 position and for further improvement of potency and physicochemical properties as well. In our results, there seem to be more space at the C-2 and C-3 position, respectively, as visualized from the Fig. 4.

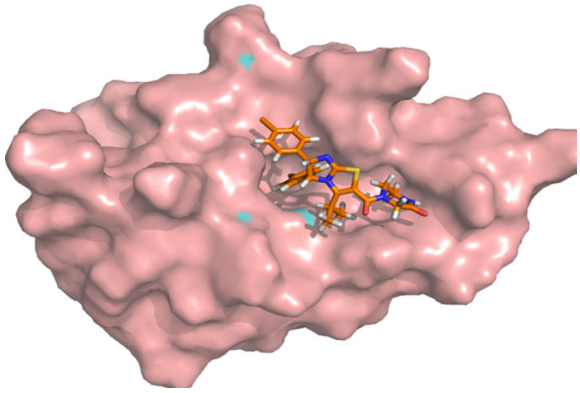

Fig. 4. Surface representation of MDM2 in complex with the compound **9c**

Binding free energies calculations: To further examine the energetics of the compound 9c to MDM2, the binding free energy was calculated by MM-GBSA method using the single trajectory protocol. The final 200 snapshots were chosen from the last 1 ns of MD trajectories for the analysis of the binding free energy. The binding free energies calculated by MM-GBSA and IC_{50} value of the inhibitor **9c** to MDM2 are -9.26 and -9.05 kcal mol^{-1}, respectively (Table-1). This clearly demonstrates that the ranking of the experimental binding free energies is in good agreement with our predictions, which shows that the current analyses by MM-GBSA method are reliable. The free energy components responsible for the calculated binding affinities are further explored. Table-1 showed that the major favorable formation of MDM2-**9c** complex is driven by the van der Waals energies. These results show that the optimizations of van der Waals interactions between the inhibitors and MDM2 may lead to the potent inhibitors of the p53-MDM2 interaction.

TABLE-1
BINDING FREE ENERGIES COMPUTED BY MM-GBSA METHOD

Components	9c + MDM2	
	Mean	std[c]
ΔG_{ele}	-4.81	2.66
ΔG_{vdw}	-38.78	4.04
ΔG_{pol}	16.27	3.44
ΔG_{nopol}	-4.63	0.25
ΔG_{gb}	-31.95	2.81
-TΔG	22.69	0.21
ΔG_{bind}	-9.26	-
ΔG_{exp}[d]	-9.05	-

All values are given in kcal mol^{-1}; Component: ΔG_{ele}: electrostatic energy in the gas phase; ΔG_{vdw}: van der Waals energy; ΔG_{nopol}: non-polar solvation energy; ΔG_{pol}: polar salvation energy; $\Delta G_{gb} = \Delta G_{vdw} + \Delta G_{nopol} + \Delta G_{ele+pol}$; -TΔS: total entropy contribution; $\Delta G_{bind} = \Delta G_{gb} - T\Delta S$; [c]Standard errors of the mean; [d]The experimental values ΔG_{exp} were derived from the experimental IC_{50} values by using the equation $\Delta G \approx -RT \ln IC_{50}$.

Inhibitor-residue interaction decomposition: In order to gain further insights into the binding mechanism of the compound **9c** to MDM2, the $\Delta G_{binding}$ is decomposed into individual residue contributions using MM-GBSA method. According to Fig. 5, the six common residues can produce the interactions of stronger than 1 kcal mol^{-1} with the compound 9c, which include Leu30, Leu33, Gly34, Ile37, Val69 and Ile75. As seen from Fig. 5, these favorable residues are focused on the hydrophobic surface cleft of the MDM2. In addition, these important residues mainly situate in the Leu26 and Trp23 subpocket, respectively.

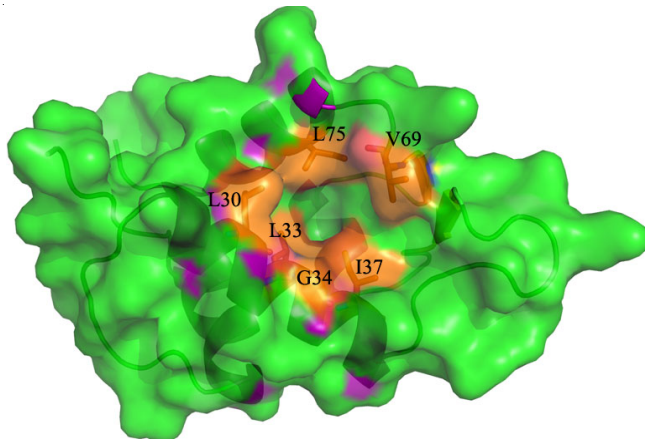

Fig. 5. Geometries of key residues, which produce some favorable interactions with the inhibitor **9c**, are plot in the complex

Conclusion

In the present study, molecular docking, molecular dynamics and MM-GBSA binding free energy calculations on the compound **9c** to MDM2 are performed to investigate the potential binding mode and to evaluate their binding affinities. The results prove that van der Waals energy drives the binding of the compound **9c** to MDM2. MD simulations reveal that two chlorophenyl groups and the *iso*-propyl group of compound **9c** are fitted with three MDM2 pockets efficiently. However, there seems to be more space and opportunity for derivatizaiton at the C-2 and C-3 position, respectively and for further improvement of potency and physicochemical properties as well. This study is expected to provide significant hints for the designs of the potent inhibitors inhibiting the p52-MDM2 interaction.

REFERENCES

1. M.B. Kastan, O. Onyekwere, D. Sidransky, B. Vogelstein and R.W. Craig, *Cancer Res*., **51**, 6304 (1991).
2. X. Wu and A.J. Levine, *Proc. Natl. Acad. Sci. USA*, **91**, 3602 (1994).
3. H. Hermeking and D. Eick, *Science*, **265**, 2091 (1994).
4. B. Vogelstein, D. Lane and A.J. Levine, *Nature*, **408**, 307 (2000).
5. K.H. Vousden and D.P. Lane, *Nat. Rev. Mol. Cell Biol*., **8**, 275 (2007).
6. A.C. Joerger and A.R. Fersht, *Annu. Rev. Biochem*., **77**, 557 (2008).
7. A. Vazquez, E.E. Bond, A.J. Levine and G.L. Bond, *Nat. Rev. Drug Discov*., **7**, 979 (2008).
8. Y. Haupt, R. Maya, A. Kazaz and M. Oren, *Nature*, **387**, 296 (1997).
9. R. Honda, H. Tanaka and H. Yasuda, *FEBS Lett*., **420**, 25 (1997).
10. M.H. Kubbutat, S.N. Jones and K.H. Vousden, *Nature*, **387**, 299 (1997).
11. W.S. el-Deiry, T. Tokino, V.E. Velculescu, D.B. Levy, R. Parsons, J.M. Trent, D. Lin, W.E. Mercer, K.W. Kinzler and B. Vogelstein, *Cell*, **75**, 817 (1993).
12. P.H. Kussie, S. Gorina, V. Marechal, B. Elenbaas, J. Moreau, A.J. Levine and N.P. Pavletich, *Science*, **274**, 948 (1996).
13. J. Momand, G.P. Zambetti, D.C. Olson, D. George and A.J. Levine, *Cell*, **69**, 1237 (1992).
14. X. Wu, J.H. Bayle, D. Olson and A.J. Levine, *Genes Dev*., **7(7a)**, 1126 (1993).
15. W. Tao and A.J. Levine, *Proc. Natl. Acad. Sci. USA*, **96**, 3077 (1999).
16. D.A. Freedman, L. Wu and A.J. Levine, *Cell. Mol. Life Sci*., **55**, 96 (1999).
17. P. Chene, *Nat. Rev. Cancer*, **3**, 102 (2003).
18. L.T. Vassilev, *J. Med. Chem*., **48**, 4491 (2005).
19. A. Ventura, D.G. Kirsch, M.E. McLaughlin, D.A. Tuveson, J. Grimm, L. Lintault, J. Newman, E.E. Reczek, R. Weissleder and T. Jacks, *Nature*, **445**, 661 (2007).
20. L.T. Vassilev, B.T. Vu, B. Graves, D. Carvajal, F. Podlaski, Z. Filipovic, N. Kong, U. Kammlott, C. Lukacs and C. Klein, *Science*, **303**, 844 (2004).
21. K. Ding, Y. Lu, Z. Nikolovska-Coleska, S. Qiu, Y. Ding, W. Gao, J. Stuckey, K. Krajewski, P.P. Roller, Y. Tomita, D.A. Parrish, J.R. Deschamps and S. Wang, *J. Am. Chem. Soc*., **127**, 10130 (2005).
22. B.L. Grasberger, T. Lu, C. Schubert, D.J. Parks, T.E. Carver, H.K. Koblish, M.D. Cummings, L.V. LaFrance, K.L. Milkiewicz, R.R. Calvo, D. Maguire, J. Lattanze, C.F. Franks, S. Zhao, K. Ramachandren, G.R. Bylebyl, M. Zhang, C.L. Manthey, E.C. Petrella, M.W. Pantoliano, I.C. Deckman, J.C. Spurlino, A.C. Maroney, B.E. Tomczuk, C.J. Molloy and R.F. Bone, *J. Med. Chem*., **48**, 909 (2005).
23. C.F. Cheok and D.P. Lane, *Drug Dev. Res*., **69**, 289 (2008).
24. H. Yin, G.- Lee, H.S. Park, G.A. Payne, J.M. Rodriguez, S.M. Sebti and A.D. Hamilton, *Angew. Chem. Int. Ed*., **44**, 2704 (2005).
25. A. Czarna, G.M. Popowicz, A. Pecak, S. Wolf, G. Dubin and T.A. Holak, *Cell Cycle*, **8**, 1176 (2009).
26. M. Liu, C. Li, M. Pazgier, C. Li, Y. Mao, Y. Lv, B. Gu, G. Wei, W. Yuan, C. Zhan, W.Y. Lu and W. Lu, *Proc. Natl. Acad. Sci. USA*, **107**, 14321 (2010).
27. C. Garcia-Echeverria, P. Chène, M.J.J. Blommers and P. Furet, *J. Med. Chem*., **43**, 3205 (2000).
28. A. Böttger, V. Böttger, S.F. Howard, S.M. Picksley, P. Chène, C. Garcia-Echeverria, H.K. Hochkeppel and D.P. Lane, *Oncogene*, **13**, 2141 (1996).
29. C. Cao, E.T. Shinohara, T.K. Subhawong, L. Geng, K.W. Kim, J.M. Albert, D.E. Hallahan and B. Lu, *Mol. Cancer Ther*., **5**, 411 (2006).
30. S. Shangary and S. Wang, *Annu. Rev. Pharmacol. Toxicol*., **49**, 223 (2009).
31. K. Ding, Y. Lu, Z. Nikolovska-Coleska, G. Wang, S. Qiu, S. Shangary, W. Gao, D. Qin, J. Stuckey, K. Krajewski, P.P. Roller and S. Wang, *J. Med. Chem*., **49**, 3432 (2006).
32. I.R. Hardcastle, J. Liu, E. Valeur, A. Watson, S.U. Ahmed, T.J. Blackburn, K. Bennaceur, W. Clegg, C. Drummond, J.A. Endicott, B.T. Golding, R.J. Griffin, J. Gruber, K. Haggerty, R.W. Harrington, C. Hutton, S. Kemp, X. Lu, J.M. McDonnell, D.R. Newell, M.E.M. Noble, S.L. Payne, C.H. Revill, C. Riedinger, Q. Xu and J. Lunec, *J. Med. Chem*., **54**, 1233 (2011).
33. S. Yu, D. Qin, S. Shangary, J. Chen, G. Wang, K. Ding, D. McEachern, S. Qiu, Z. Nikolovska-Coleska, R. Miller, S. Kang, D. Yang and S. Wang, *J. Med. Chem*., **52**, 7970 (2009).
34. I.R. Hardcastle, S.U. Ahmed, H. Atkins, G. Farnie, B.T. Golding, R.J. Griffin, S. Guyenne, C. Hutton, P. Källblad, S.J. Kemp, M.S. Kitching, D.R. Newell, S. Norbedo, J.S. Northen, R.J. Reid, K. Saravanan, H.M. Willems and J. Lunec, *J. Med. Chem*., **49**, 6209 (2006).
35. J.G. Allen, M.P. Bourbeau, G.E. Wohlhieter, M.D. Bartberger, K. Michelsen, R. Hungate, R.C. Gadwood, R.D. Gaston, B. Evans, L.W. Mann, M.E. Matison, S. Schneider, X. Huang, D. Yu, P.S. Andrews, A. Reichelt, A.M. Long, P. Yakowec, E.Y. Yang, T.A. Lee and J.D. Oliner, *J. Med. Chem*., **52**, 7044 (2009).
36. P. Furet, P. Chène, A. De Pover, T.S. Valat, J.H. Lisztwan, J. Kallen and K. Masuya, *Bioorg. Med. Chem. Lett*., **22**, 3498 (2012).
37. S.Y. Lu, Y.J. Jiang, J.W. Zou and T.X. Wu, *J. Mol. Graph. Model*., **30**, 167 (2011).
38. A.M. Almerico, M. Tutone, L. Pantano and A. Lauria, *Biochem. Biophys. Res. Commun*., **424**, 341 (2012).
39. H.S. Lee, S. Jo, H.S. Lim and W. Im, *J. Chem. Inf. Model*., **52**, 1821 (2012).
40. J. Chen, D. Zhang, Y. Zhang and G. Li, *Int. J. Mol. Sci*., **13**, 2176 (2012).
41. M. Miyazaki, H. Kawato, H. Naito, M. Ikeda, M. Miyazaki, M. Kitagawa, T. Seki, S. Fukutake, M. Aonuma and T. Soga, *Bioorg. Med. Chem. Lett*., **22**, 6338 (2012).
42. W. Wang, W.A. Lim, A. Jakalian, J. Wang, J. Wang, R. Luo, C.I. Bayly and P.A. Kollman, *J. Am. Chem. Soc*., **123**, 3986 (2001).
43. W. Wang and P.A. Kollman, *J. Mol. Biol*., **303**, 567 (2000).
44. J. Wang, P. Morin, W. Wang and P.A. Kollman, *J. Am. Chem. Soc*., **123**, 5221 (2001).
45. Y. Tong, Y. Mei, Y.L. Li, C.G. Ji and J.Z. Zhang, *J. Am. Chem. Soc*., **132**, 5137 (2010).
46. J. Chen, S. Zhang, X. Liu and Q. Zhang, *J. Mol. Model*., **16**, 459 (2010).
47. E.L. Wu, K.L. Han and J.Z.H. Zhang, *Chem. Eur. J*., **14**, 8704 (2008).
48. T. Hou and R. Yu, *J. Med. Chem*., **50**, 1177 (2007).
49. Y. Xu and R. Wang, *Proteins*, **64**, 1058 (2006).
50. B. Kuhn, P. Gerber, T. Schulz-Gasch and M. Stahl, *J. Med. Chem*., **48**, 4040 (2005).
51. J.Z. Chen, M.Y. Yang, C.H. Yi, S.H. Shi and Q.G. Zhang, *J. Mol. Struct. THEOCHEM*, **899**, 1 (2009).
52. J.M.J. Swanson, R.H. Henchman and J.A. McCammon, *Biophys. J*., **86**, 67 (2004).
53. G. Hu, D. Wang, X. Liu and Q. Zhang, *J. Comput. Aided Mol. Des*., **24**, 687 (2010).
54. The PyMOL Molecular Graphics System, Version 0.99.
55. G.M. Morris, R. Huey, W. Lindstrom, M.F. Sanner, R.K. Belew, D.S. Goodsell and A.J. Olson, *J. Comput. Chem*., **30**, 2785 (2009).
56. D.A. Case, T.A. Darden, T.E. Cheatham, I.C.L. Simmerling, J. Wang, R.E. Duke, R. Luo, M. Crowley, R.C. Walker, W. Zhang, K.M. Merz, B. Wang, S. Hayik, A. Roitberg, G. Seabra, I. Kolossváry, K.F. Wong, F. Paesani, J. Vanicek and X. Wu, S.R Brozell, T. Steinbrecher, H. Gohlke, L. Yang, C. Tan, J. Mongan, V. Hornak, G. Cui, D.H. Mathews, M.G. Seetin, C. Sagui, V. Babin and P.A. Kollman, AMBER 12, University of California, San Francisco (2012).
57. B. Kuhn, P.A. Kollman and M. Stahl, *J. Comput. Chem*., **25**, 1865 (2004).
58. T.G. Coleman, H.C. Mesick and R.L. Darby, *Ann. Biomed. Eng*., **5**, 322 (1977).
59. T. Darden, D. York and L. Pedersen, *J. Chem. Phys*., **98**, 10089 (1993).
60. U. Essmann, L. Perera, M.L. Berkowitz, T. Darden, H. Lee and L.G. Pedersen, *J. Chem. Phys*., **103**, 8577 (1995).